

PERFORMANCE OF 1-m LONG / 75-mm BORE SUPERCONDUCTING PROTOTYPE COILS FOR HERA

G.Horlitz, H.Kaiser, G.Knust, K.-H.Mess, and S.Wolff
DESY, Hamburg, W. Germany

P.Schlüser

II. Inst. für Experimentalphysik, Univ. Hamburg, W.Germany

B.H.Wiik

II. Inst. für Experimentalphysik, Univ. Hamburg, and DESY, Hamburg, W.Germany.

Abstract

Two short prototypes of the new HERA superconducting dipole magnets with 75 mm inner bore have been built and tested in a bath cryostat. Both coils have reached the short sample current of the cable after a few training steps. The quench current depends linearly on the temperature between 4.0 and 5.0 K. The field quality of both coils is in general within specifications. There is no current dependence of the higher harmonics except for the well-known hysteresis due to persistent currents.

Introduction

The proposed electron proton storage ring HERA¹ requires superconducting dipoles, quadrupoles and correction elements for acceleration and storage of 820 GeV protons.

At the time of the ECFA study for HERA (1980), the only successful concept suitable for mass production of superconducting magnets was that of the Energy Saver magnet at Fermilab². Many principles of this concept have therefore been adopted.

Following the concept of the first ECFA study, three warm bore, warm yoke prototype dipoles of reduced length (1 m) with 100 mm inner coil diameter and 4.73 T nominal central induction were built and tested successfully³.

Meanwhile, a review of the proposal has resulted in major changes of the concept⁴, mainly for cost reasons. The new design contains cold bore, warm yoke magnets of 75 mm inner coil diameter, 4.53 T nominal induction and 6.08 m effective magnetic length.

Before producing full size prototypes, two coils of 1 m length have been fabricated and tested.

General Magnet Description

A cross section through the magnet is shown in Fig. 1. The main parameters are listed in Table I.

Table I - Main magnet parameters

central nominal induction	B_0	=	4.53 T
central nominal induction without yoke	B_{co}	=	4.09 T
max. induction in conductor with yoke	B_{max}	=	4.915 T
nominal current	I_n	=	5669 A
number of turns	n	=	102
inner coil diameter	d	=	0.075 m
inner yoke diameter	d_{Fe}^c	=	0.277 m
iron yoke width	w_{Fe}	=	0.500 m
iron yoke height	h_{Fe}	=	0.380 m

The main features of the magnet are: two coil shells clamped by stainless steel collars and embedded in one phase helium; a two phase helium return path for heat exchange; insulating vacuum and heat shield at 50 K; a warm iron yoke.

The Conductor

The coils are wound from a keystone Rutherford type cable with specified parameters as listed in Table II. Each of the 24 strands in the cable is covered

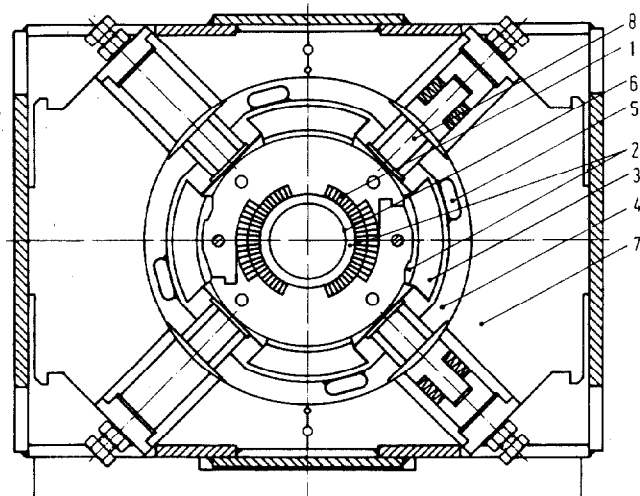


Fig. 1 - Magnet cross section. Coil (1), one phase helium (2), two phase helium (3), insulating vacuum (4), shield cooling gas (5), beam vacuum tube (6), iron yoke (7), coil support (8).

with a 0.005 mm thick silver tin layer (5% Ag, 95% Sn). The cable compaction factor is 0.90 so 10% of the space in the cable is expected to be filled with liquid helium.

Two different types of insulation have been used (see Fig. 2). In both types a first layer of a 12 mm wide and 0.025 mm thick Kapton tape is wrapped around the cable with 60% overlap. The first coil, labelled 1S1, has a second insulation layer of 0.075 mm thick and 9 mm wide Kapton tape wrapped around the cable with 1 mm gaps between adjacent turns. The tape is covered on both sides with Thermibond*, a polymerized polyimide glue with a curing temperature of 180°C.

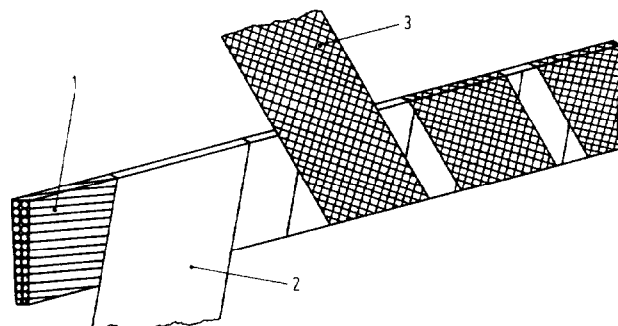


Fig. 2 - Cable insulation. Rutherford type cable (1), Kapton layer (2), Kapton with Thermibond for coil 1S1 or 8-stage impregnated glass fibre tape for coil 1S2 (3).

In the second coil, 1S2, the second insulation layer consists of 0.12 mm thick and 9 mm wide glass fibre

* Schweizerische Isola-Werke, Breitenbach, Switzerland.

tape filled with 24% B stage epoxy to be cured at 160°C. Here the gaps between adjacent turns are 3 mm.

Table II - Conductor parameters

cable height	$h = 10.00 \pm 0.03$ mm
cable inner width	$w_1 = 1.28 \pm 0.02$ mm
cable outer width	$w_2 = 1.67 \pm 0.02$ mm
number of strands	$n_s = 24$
strand diameter, untinned	$d_s = 0.83 \pm 0.01$ mm
copper/superconductor ratio	$\alpha_s = 1.8 \pm 0.1$
diameter of filaments	$d_f = 0.010 \pm 0.002$ mm
number of filaments	$n_f \sim 2460$
filament twist pitch	$p_f = 25$ mm
cable twist pitch	$p_c \leq 120$ mm
nominal operating current	$I_n = 5669$ A
critical short sample current in cable at $T = 4.6$ K and $B = 5.5$ T	$I_{cr,s} = 6318$ A**

** It should be noted that coil 1S2 and one half coil of 1S1 have been wound with cables with a few per-cent lower critical current.

The Coil

A more detailed cross section of the coil is shown in Fig. 3. The upper and lower half coils are fabricated separately. There are 32 turns in the inner and 19 turns in the outer half coil. At the ends of the inner coil, 25 mm wide spacers of glass fibre reinforced epoxy (G11) are placed behind turns 1, 3 and 9 in order to avoid a field enhancement⁵. The cured inner half coil is covered by a 0.5 mm thick G11 layer with slots for helium penetration. The outer half coil is wound and cured on top of this. To assure high cross sectional accuracy, both the winding mandrel and the curing molds are made from punched laminations.

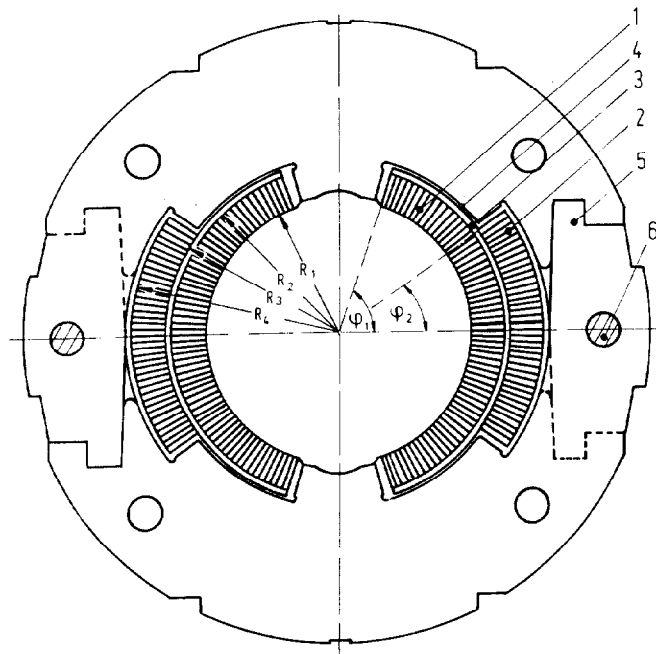


Fig. 3 - Coil cross section. Inner coil layer (1), outer coil layer (2), intermediate banding (3), coil insulation (4), stainless steel collars (5), longitudinal rods (6), $R_1 = 37.50$ mm, $R_2 = 47.76$ mm, $R_3 = 48.25$ mm, $R_4 = 58.51$ mm, $\phi_1 = 71.895^\circ$, $\phi_2 = 35.117^\circ$ (for coil 1S1).

The overall length of coils 1S1 and 1S2 is 0.98 m, the length of the straight coil sections is 0.78 m.

The upper and lower half coils are assembled on a cylindrical mandrel and insulated with 6 layers of 0.125 mm thick Kapton. 10 cm long packs of laminated

stainless steel clamps are placed around the coil from top and bottom, interlacing each other like combs. These collars are then pressed together in a large hydraulic press until 10 mm thick rods can be fitted through in the medium plane to lock the collars. This design allows to open the collars without destruction if a reshimming of the coil should be necessary. A force of about 450 tons has been applied to close the collars of the 1 m long coils.

Test Results

Both coils have been tested in a vertical helium bath cryostat to measure the quench behaviour and the field quality.

The first quench tests have been made at a fixed temperature of 4.6 K. Both coils showed some training (3 steps for 1S1, 11 steps for 1S2 to reach the design current).

The maximum quench current is plotted in Fig. 4 as a function of temperature. The data show the expected linear dependence except for temperatures below 4 K where the magnetic forces are more than 40% above the nominal values. At 3.9 K the maximum currents are 7160 A for coil 1S1 and 7240 A for coil 1S2 corresponding to a central induction of 5.16 T and 5.22 T, respectively.

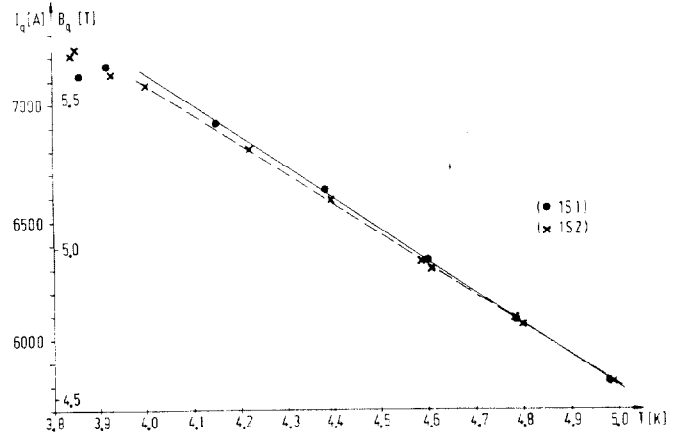


Fig. 4 - Quench current versus temperature. B_q = maximum induction at conductor = $1.085 \cdot B_0$.

The magnetic field has been measured with a 0.3 m long system of radially arranged coils rotating slowly around the symmetry axis. The field quality can be characterized in terms of the harmonic coefficients b_n for normal multipole fields and a_n for skew multipole fields. These coefficients are obtained from the Fourier expansion of the azimuthal field component

$$B(r, \phi) = B_0 \sum_{n=1}^{\infty} \left(\frac{r}{r_0} \right)^{n-1} (b_n \cos n\phi - a_n \sin n\phi)$$

B_0 is the induction on the axis and $r_0 = 2.5$ cm the reference radius.

Before starting the field measurements the current was ramped up to 6000 A and down to zero again. The measurements of the harmonics have been performed at a number of different currents along a second complete cycle.

The harmonic coefficients as measured at 6000 A are listed in Table III and compared with the design values. The differences are in general small and tolerable. The rather large 14- and 18-pole coefficients are an inherent feature of a homogeneous two-layer coil. In future magnets they will be eliminated by wedges in both coil layers.

Table III - Straight section harmonics without iron yoke (at $r = 2.5$ cm, relative to B_0) at 6000 A

harmonic no. n	design values $b_n \times 10^4$	coil 1S1 $b_n \times 10^4$	1S1 $a_n \times 10^4$	coil 1S2 $b_n \times 10^4$	1S2 $a_n \times 10^4$
1	10000.				
2	0.	-0.5	4.3	-2.3	-0.7
3	-1.1, 7.8*	-1.0	0.2	7.9	-0.2
4	0.	0.3	0.0	-0.7	-0.6
5	0.	-0.7	0.0	-1.2	0.3
6	0.	-0.4	0.7	0.2	0.4
7	14.9	14.1	-0.6**	14.5	-0.4**
8	0.	0.0**	0.0**	0.0**	0.0**
9	-13.2	-12.6	0.5	-11.8	0.3

* design value -1.1 for 1S1, 7.8 for 1S2,

** used for off center correction of the measuring coil system.

The current dependence of the quadrupole and sextupole coefficients is shown in Fig. 5. Coil 1S1 has a somewhat high skew quadrupole coefficient which shows a hysteresis at low currents. The reason may be that the upper and lower half coil have been wound from cables with different critical currents. The nor-

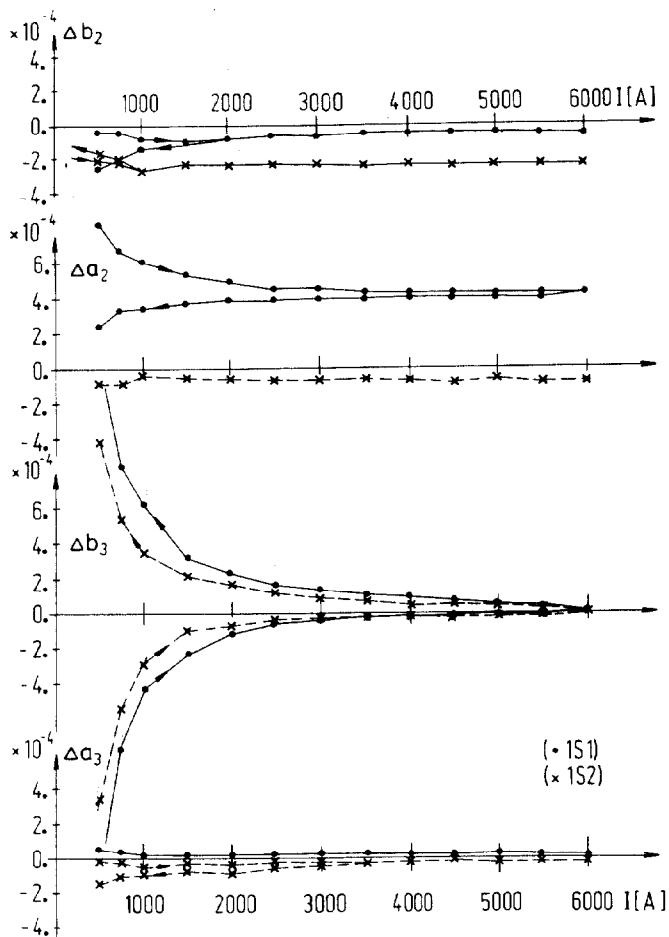


Fig. 5 - Straight section harmonics without iron yoke. Deviations of normal harmonics Δb_2 (quadrupole) and Δb_3 (sextupole) and skew harmonics Δa_2 and Δa_3 from design values ($b_2 = a_2 = a_3 = 0$, $b_3 = -1.1 \times 10^{-4}$ for coil 1S1 and $b_3 = 7.8 \times 10^{-4}$ for coil 1S2) versus current.

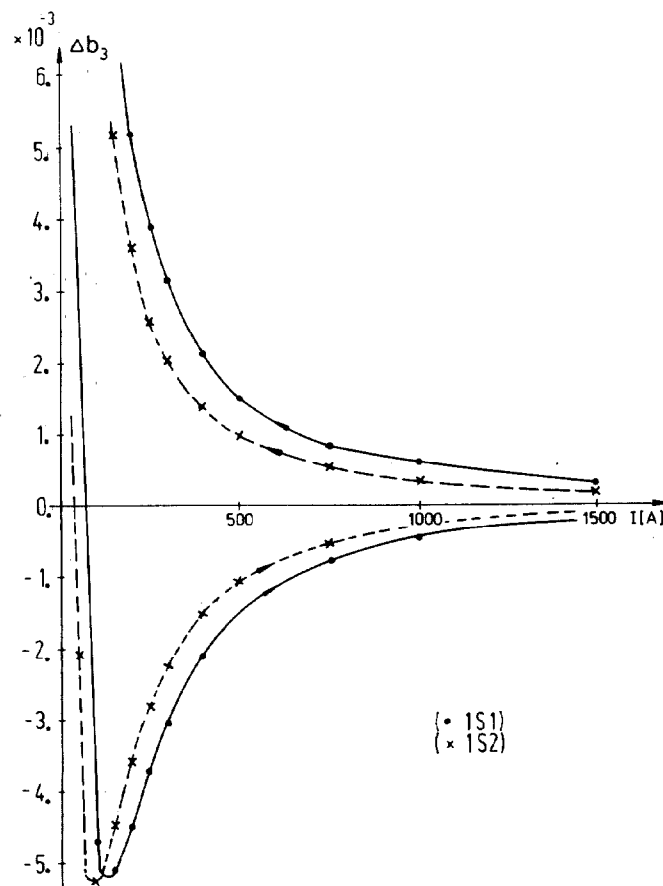


Fig. 6 - Persistent current sextupole without iron yoke. Hysteresis during up and down ramping of current.

mal sextupole b_3 shows the well-known hysteresis due to persistent currents. This is seen more clearly in Fig. 6. There is a slight shift between the curves of 1S1 and 1S2 which may also be due to the different conductors used.

The harmonic coefficients are constant at high currents. This proves that the coils are clamped with sufficient precompression.

Acknowledgements

We would like to express our gratitude to all technicians, engineers and scientists who have contributed to the design, fabrication and tests of these magnets.

References

1. "Study on the Proton-Electron Storage Ring Project HERA, Report of the electron proton working group of ECFA", ECFA80/42 (DESY HERA 80/01), March 17, 1980.
2. "A Report on the Design of the Fermi National Accelerator Laboratory Superconducting Accelerator", FNAL Design Report, May 1979.
3. G.Horlitz, S.Wolff, "Performance of 1 m long / 100 mm Bore Superconducting Dipole Prototypes for HERA", Proc. Appl. Supercond. Conf., Knoxville, 1982 (to be published), preprint: DESY HERA 82/12, December 1982.
4. "HERA, a Proposal for a Large Electron-Proton Colliding Beam Facility at DESY", DESY HERA 81/10, July 1981.
5. D.Hochman, "End-Field Design for HERA Superconducting Dipoles", DESY HERA 82/03, March 1982.